

UNCLASSIFIED

SECURITY CLASSIFICATION OF THIS PAGE (When Data Entered)

REPORT DOCUMENTATION PAGE		READ INSTRUCTIONS BEFORE COMPLETING FORM
1. REPORT NUMBER	2. GOVT ACCESSION NO.	3. RECIPIENT'S CATALOG NUMBER
4. TITLE (and Subtitle) ATTENUATION OF EMP IN THE WAVE ZONE DUE TO IMPERFECTLY CONDUCTING GROUND		5. TYPE OF REPORT & PERIOD COVERED Topical Report
		6. PERFORMING ORG. REPORT NUMBER MRC-R-400
7. AUTHOR(s) Conrad L. Longmire		8. CONTRACT OR GRANT NUMBER(s) DNA001-78-C-0141
9. PERFORMING ORGANIZATION NAME AND ADDRESS MISSION RESEARCH CORPORATION 735 State Street, P. O. Drawer 719 Santa Barbara, California 93102		10. PROGRAM ELEMENT, PROJECT, TASK AREA & WORK UNIT NUMBERS NWED62704H R99QAXEA091-82
11. CONTROLLING OFFICE NAME AND ADDRESS Director DEFENSE NUCLEAR AGENCY Washington, D. C. 20305		12. REPORT DATE June 1978
		13. NUMBER OF PAGES
14. MONITORING AGENCY NAME & ADDRESS (if different from Controlling Office)		15. SECURITY CLASS (of this report) Unclassified
		15a. DECLASSIFICATION, DOWNGRADING SCHEDULE
16. DISTRIBUTION STATEMENT (of this Report)		
17. DISTRIBUTION STATEMENT (of the abstract entered in Block 20, if different from Report)		
18. SUPPLEMENTARY NOTES		
19. KEY WORDS (Continue on reverse side if necessary and identify by block number) Electromagnetic Pulse Radiated EMP Effects of Nuclear Explosions		
20. ABSTRACT (Continue on reverse side if necessary and identify by block number) Previously, EMP fields from nuclear surface bursts have been extrapolated to points far beyond the source region by use of a multipole extrapolation based on perfect ground conductivity. This report presents a method for correcting the extrapolated fields to account for actual ground impedance. The method is shown to compare favorably with Sommerfeld's solution for a dipole radiating over a flat earth.		

CONTENTS

	PAGE
ILLUSTRATIONS	2
SECTION	
1 INTRODUCTION AND SUMMARY	3
2 THE DIFFRACTION EQUATION IN THE AIR	4
3 FIELDS IN THE GROUND	8
4 THE SCALED EQUATIONS	10
5 INTEGRAL EQUATION FOR F_1	15
6 APPROXIMATE SOLUTION OF THE INTEGRAL EQUATION	17
7 ACCURATE SOLUTION OF THE INTEGRAL EQUATION	19
8 RESULTS IN TIME DOMAIN	23
9 COMPARISON WITH SOMMERFELD SOLUTION	25
10 HORIZONTAL ELECTRIC FIELD	28
REFERENCES	20

ILLUSTRATIONS

FIGURE		PAGE
1	Dependence of F on y and T . Dashed lines show where F extrapolates to zero.	12
2.	Comparison of various approximations to F . Solid curves, Longley's computed results. Dashed curves, approximate theoretical result, Equation 72. Circles, computed from fit, Equation 73.	22
3	Comparison with Sommerfeld's results. Solid curve, Norton's evaluation of Sommerfeld's results, Equation 81. Dashed curve, our approximate theoretical result, Equation 87. Note that relation of dashed to solid curve is very nearly the same as in Figure 2.	26

SECTION 1 INTRODUCTION AND SUMMARY

Present computer codes for calculating the electromagnetic pulse (EMP) from nuclear bursts on or near the air-ground interface ignore the effect of finite ground conductivity in extrapolating the EMP to distances far outside the source region. Both the MRC codes LEMP-SUBL (References 1 and 2) and the AFWL code SCX (Reference 3) include finite ground conductivity within the computational mesh, but fields outside the outer boundary (typically chosen a few kilometers from the burst point) are calculated in terms of an outgoing multipole expansion which is based on the assumption of a perfectly conducting ground.

However, it is known that, for observers on the ground, the higher frequencies in the radiated EMP are attenuated in distances of the order of tens of kilometers, and the lower frequencies in somewhat longer distances.

In this report we derive a simple way of correcting the extrapolated fields to include the attenuation due to imperfectly conducting ground. Predictions from this simple but approximate method are compared with exact results of Sommerfeld for a dipole radiating over a flat earth, and are shown to be of good accuracy relative to unavoidable uncertainties in practical situations.

SECTION 2
THE DIFFRACTION EQUATION IN THE AIR

We use the standard spherical coordinates r, θ, ϕ , right handed in the order given, with origin on the ground at the burst point and the $\theta = 0$ axis vertical. We have electric field components E_r and E_θ and magnetic field component B_ϕ . We are interested in solving Maxwell's equations in the air outside the source region, where the Compton current and air conductivity are negligible. Maxwell's equations become, in cgs Gaussian units,

$$\frac{1}{c} \frac{\partial E_r}{\partial t} = \frac{1}{r \sin \theta} \frac{\partial}{\partial \theta} \sin \theta B_\phi, \quad (1)$$

$$\frac{1}{c} \frac{\partial E_\theta}{\partial t} = -\frac{1}{r} \frac{\partial}{\partial r} r B_\phi, \quad (2)$$

$$\frac{1}{c} \frac{\partial B_\phi}{\partial t} = -\frac{1}{r} \frac{\partial}{\partial r} r E_\theta + \frac{1}{r} \frac{\partial}{\partial \theta} E_r. \quad (3)$$

As usual in EMP problems, it is convenient to think of the fields as functions of retarded time τ , i.e.,

$$E_r = E_r(\tau, r, \theta), \text{ etc.}, \quad (4)$$

where

$$\tau \equiv ct - r = \text{retarded time in length units}. \quad (5)$$

It is also convenient to replace E_θ and B_ϕ by the outgoing and ingoing fields

$$\left. \begin{aligned} F &= r(E_\theta + B_\phi), & E_\theta &= (F+G)/2r, \\ G &= r(E_\theta - B_\phi), & B_\phi &= (F-G)/2r. \end{aligned} \right\} \quad (6)$$

The Equations 1, 2, and 3 become

$$\frac{\partial E_r}{\partial \tau} = \frac{1}{2r^2 \sin\theta} \frac{\partial}{\partial \theta} \sin\theta (F-G) , \quad (7)$$

$$\frac{\partial F}{\partial r} = \frac{\partial}{\partial \theta} E_r , \quad (8)$$

$$2 \frac{\partial G}{\partial \tau} - \frac{\partial G}{\partial r} = - \frac{\partial}{\partial \theta} E_r . \quad (9)$$

The exact solutions of these equations are the multipole fields. The outgoing multipole fields of order $\ell =$ odd integer, which have $E_r = 0$ at $\theta = \pi/2$ (the ground surface), have been used in LEMP-SUBL and SCX to extrapolate the fields over perfectly conducting ground.

In the wave zone ($r \gg$ wavelength considered), F is the dominant field. For example, for a dipole field we try

$$F \approx A(\tau) \sin\theta \quad \text{independent of } r , \quad (10)$$

we find from Equation 7,

$$E_r \approx \frac{\cos\theta}{r^2} \int A d\tau , \quad (11)$$

and from Equation 9,

$$G \approx \frac{\sin\theta}{2r^2} \int d\tau \int A d\tau . \quad (12)$$

Equation 8 then leads to higher inverse powers of r in F . Thus E_r and G fall off as $1/r^2$, while F is independent of r to first order.

When finite ground conductivity is considered, we shall see that F goes eventually as $1/r$, while E_r and G still go as $1/r^2$. This means that E_r and F give terms of the same order in Equation 8, so that E_r cannot be neglected ($E_r \times B_\phi$ feeds energy into the ground). However, G is still of higher order than F , and can be neglected.

We choose $\tau = 0$ to be at the beginning of the EMP, true at all radii. The fields then vanish for $\tau < 0$, and we may use the Laplace transform. Multiplying Equations 7 and 8 by $\exp(-s\tau)$ and integrating on τ from 0 to ∞ , we obtain

$$sE_r = \frac{1}{2r^2 \sin\theta} \frac{\partial}{\partial\theta} \sin\theta F, \quad (13)$$

$$\frac{\partial F}{\partial r} = \frac{\partial}{\partial\theta} E_r, \quad (14)$$

where F and E_r are now the Laplace transforms of the time-dependent fields. Note that the Laplace variable s has the dimensions of an inverse length, and is the inverse of the (reduced) wavelength $\lambda = \lambda/2\pi$.

Equations 13 and 14 can be combined to eliminate either F or E_r . Before doing this we note that finite ground conductivity will affect the fields only at angles quite close to $\theta = \pi/2$, near the ground surface, as we shall verify later. In this case, $\sin\theta$ can be replaced by unity in Equation 13, and we obtain from (14)

$$\frac{\partial F}{\partial r} = \frac{1}{2r^2 s} \frac{\partial^2 F}{\partial\theta^2}, \quad (15)$$

after eliminating E_r , which is in turn to be determined from (13), or

$$E_r = \frac{1}{2r^2 s} \frac{\partial F}{\partial\theta}. \quad (16)$$

Equation 15 has the form of a diffusion equation. Actually, the process it describes is diffraction. As F is absorbed at the ground by finite ground conductivity, more F is supplied from the region farther above the ground by diffraction.

If the ground were perfectly conducting, we would have $E_r = 0$ at $\theta = \pi/2$. Then according to Equation 16, we would have $\partial F/\partial\theta = 0$ there. The solution of Equation 15 would then be

$$F = F(s) = \text{independent of } r \text{ and } \theta . \quad (17)$$

This is the same as Equation 10 for θ near $\pi/2$.

For application to LEMP-SUBL, we shall want to solve Equation 15 from $r = r_0$ outwards, where r_0 is the outer boundary of the LEMP-SUBL computational mesh. We shall want to start at $r = r_0$ with $F = F_0$, the field provided by LEMP-SUBL. If we can solve our present problem for F_0 an impulse function, then the solution for an actual LEMP-SUBL problem will be a convolution of the impulse solution with the F_0 given by LEMP-SUBL. Accordingly, we take F_0 to be the impulse function

$$F_0(\tau, \theta) = \delta(\tau) = \text{independent of } \theta. \quad (18)$$

For the Laplace transform field we then have

$$F_0(s, \theta) = 1 . \quad (19)$$

Now the F_0 provided by LEMP-SUBL is not independent of θ , and varies somewhat over the region of θ near $\pi/2$ that will be affected by the finite ground conductivity. However, the multipole extrapolation procedure used in LEMP-SUBL already correctly handles the diffraction resulting from that angular variation, over a perfectly conducting ground. Our desire here is to correct the extrapolated fields only for ground-induced attenuation. Thus we want to look for solutions which would have no diffraction if it were not for finite ground conductivity, i.e., we want to look for solutions starting with the form (18) and (19).

SECTION 3
FIELDS IN THE GROUND

The fields in the ground propagate nearly in the vertically downward direction, because the index of refraction there is large compared with unity. Thus in the ground we consider only E_r and B_ϕ , which satisfy

$$\frac{\epsilon}{c} \frac{\partial E_r}{\partial t} + 4\pi\sigma E_r = \frac{\partial}{\partial z} B_\phi, \quad (20)$$

$$\frac{1}{c} \frac{\partial B_\phi}{\partial t} = \frac{\partial}{\partial z} E_r. \quad (21)$$

Here the coordinate z increases downward, as does θ above the ground. Going to retarded time and again taking the Laplace transform, we obtain

$$(\epsilon s + 4\pi\sigma) E_r = \frac{\partial}{\partial z} B_\phi, \quad (22)$$

$$s B_\phi = \frac{\partial}{\partial z} E_r. \quad (23)$$

It is easy to see that the desired solution of these equations is

$$E_r = E_\theta e^{-kz}, \quad B_\phi = B_\theta e^{-kz}, \quad (24)$$

where

$$k = +\sqrt{s(\epsilon s + 4\pi\sigma)}. \quad (25)$$

Equation 23, evaluated at the ground surface, then provides a relation between E_r and B_ϕ ,

$$\begin{aligned}
E_r &= -\frac{s}{k} B_\phi \text{ at surface ,} \\
&= -\frac{s}{2rk} F \text{ at surface .}
\end{aligned}
\tag{26}$$

The second equation here comes from Equation 6 when G is negligible. Combining this result with Equation 16, we obtain a boundary condition on F at the ground surface,

$$\frac{\partial F}{\partial \theta} = \frac{rs^2}{k} F \text{ at } \theta = \frac{\pi}{2} .
\tag{27}$$

The propagation direction in the ground is not exactly vertical. If the field E_z is included and the driving field at $z = 0$ is assumed to be a function only of $\tau = ct - r$, but if terms of order $1/sr = \lambda/r$ are neglected compared with unity in Maxwell's equations, then it can be shown that Equation 25 for k is replaced by

$$k = +\sqrt{s[(\epsilon-1)s + 4\pi\sigma]} .
\tag{28}$$

Since in typical soils $\epsilon \gtrsim 10$, the difference between Equations 28 and 25 is negligible. The analysis that led to Equation 28 also gives a relation between E_z and E_r ,

$$E_z \approx -\sqrt{\frac{s}{(\epsilon-1)s + 4\pi\sigma}} E_r \text{ (in ground) .}
\tag{29}$$

E_z is usually small compared with E_r .

SECTION 4
THE SCALED EQUATIONS

The diffraction Equation 15 for F , the starting form (19) for the impulse solution, and the boundary condition (27) are sufficient to determine the solution. Before discussing the solution, we shall scale the variables to reduce the number of parameters in the equations to the minimum possible.

Since r ranges from r_0 to ∞ , we replace r by

$$x \equiv r/r_0, \quad 1 \leq x \leq \infty. \quad (30)$$

Equation 15 then becomes

$$x^2 \frac{\partial F}{\partial x} = \frac{1}{2r_0 s} \frac{\partial^2 F}{\partial \theta^2}. \quad (31)$$

We can eliminate all parameters from this equation if we replace θ by

$$y = (\frac{\pi}{2} - \theta)/\delta\theta, \quad \delta\theta \equiv 1/\sqrt{sr_0} = \sqrt{\frac{\lambda}{r_0}}. \quad (32)$$

We then have

$$x^2 \frac{\partial F}{\partial x} = \frac{1}{2} \frac{\partial^2 F}{\partial y^2}, \quad F(1, y) = 1. \quad (33)$$

The starting form (19) of F is unchanged, and the boundary condition (27) becomes

$$\frac{\partial F}{\partial y} = \beta x F \quad \text{at} \quad y = 0, \quad (34)$$

where β is the dimensionless parameter

$$\beta \equiv s \sqrt{\frac{r_0}{\epsilon s + 4\pi\sigma}} \equiv sD = \frac{D}{\lambda}. \quad (35)$$

Here D is a length that usually will depend only slowly on s , and we shall later regard it as constant.

Equation 33 can be converted into the standard diffusion equation by replacing the variable x by

$$T = 1 - \frac{1}{x}, \quad 0 \leq T \leq 1. \quad (36)$$

Then $dT = dx/x^2$, and we obtain

$$\frac{\partial F}{\partial T} = \frac{1}{2} \frac{\partial^2 F}{\partial y^2}, \quad F(0, y) = 1. \quad (37)$$

Since the range of the variable T is finite and equal to unity, this form shows that the range of y over which the ground can affect F is limited to $y \lesssim 1$, or

$$\frac{\pi}{2} - \theta \lesssim \delta\theta. \quad (38)$$

For large s or short λ , $\delta\theta$ is small according to Equation 32.

In terms of T , the boundary condition (34) becomes

$$\frac{\partial F}{\partial y} = \frac{\beta}{1-T} F \text{ at } y = 0. \quad (39)$$

It is easy now to see what the qualitative nature of the solution will be. The graphical interpretation of the boundary condition (39) is that F will vanish if extrapolated linearly from $y = 0$ to $y = -\delta y$, where

$$\delta y = \frac{F}{\partial F / \partial y} = \frac{(1-T)}{\beta}. \quad (40)$$

The extrapolation distance δy goes to zero as T approaches unity. The behavior of F is therefore as sketched in Figure 1, which has been drawn

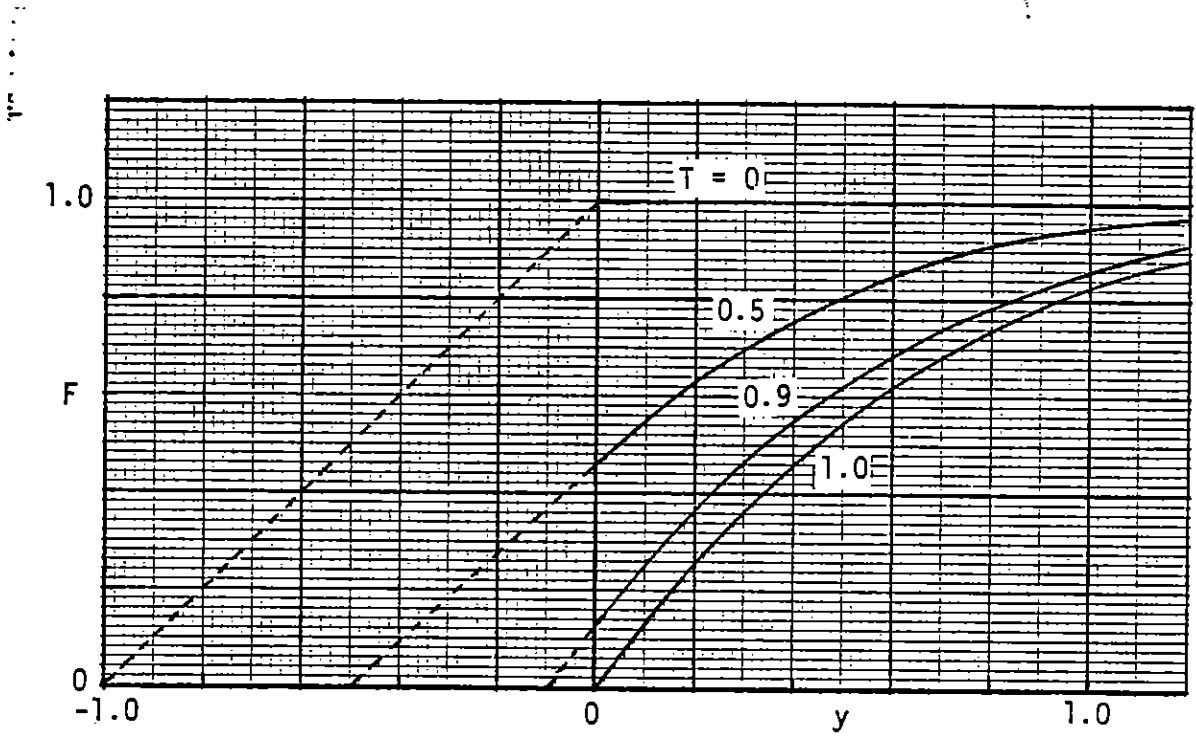


Figure 1. Dependence of F on y and T . Dashed lines show where F extrapolates to zero.

for the case $\beta = 1$. The boundary condition forces F to have a finite slope at $y = 0$, but the slope goes to zero at large y . The curvature of F is thus negative, and therefore, according to Equation 37, F decreases with T at all y .

We can use this picture to make plausible guesses as to the behavior with T of the value F_1 of F at $y = 0$. First, for $T \ll 1$, it is plausible that F_1 will fall in such a way that $(1-F_1) \sim \sqrt{T}$. Since for F near unity and $1-T$ also near unity, Equation 39 indicates $\partial F/\partial y \sim \beta$, it is reasonable to expect that

$$\left. \begin{aligned} F_1 &\approx 1 - \text{constant} \times \beta \sqrt{T} \\ &\approx 1 - \text{constant} \times \beta \sqrt{x-1} \end{aligned} \right\} \text{ for } T \ll 1. \quad (41)$$

We shall verify this expectation later and evaluate the constant.

Next, consider the limit as $T \rightarrow 1$ ($x \rightarrow \infty$). If the slope $\partial F/\partial y$ approaches a constant value F' at $y = 0$ in this limit, then Equation 39 shows that

$$F_1 \rightarrow \frac{1-T}{\beta} F' = \frac{1}{\beta x} F' \quad \text{as } x \rightarrow \infty. \quad (42)$$

This indicates that F_1 decreases linearly with T . According to Equation 37, F_1 can decrease linearly with T if the curvature $\partial^2 F/\partial y^2$ is approximately constant in T near $y = 0$. It is in fact plausible that both F' and the curvature approach constant values as $T \rightarrow 1$. Now, how does F' depend on β ? For smaller β , Equation 40 shows that the extrapolation distance goes to zero faster as $T \rightarrow 1$, and there is therefore less time (T) for F to decrease at points $y > 0$. Thus we expect F' to increase (at $T \approx 1$) as β decreases, and a plausible guess is that $F' \sim 1/\beta$. Equation 42 then becomes

$$\begin{aligned}
 F_1 &\rightarrow \text{constant} \times \frac{1 - T}{\beta^2} \\
 &\rightarrow \text{constant} \times \frac{1}{\beta^2 x}
 \end{aligned}
 \left. \vphantom{\begin{aligned} F_1 &\rightarrow \text{constant} \times \frac{1 - T}{\beta^2} \\ &\rightarrow \text{constant} \times \frac{1}{\beta^2 x} \end{aligned}} \right\} \text{as } x \rightarrow \infty . \quad (43)$$

We shall also verify this result and evaluate the constant.

SECTION 5
INTEGRAL EQUATION FOR F_1

We can eliminate the y variable and obtain an integral equation for F_1 , the value of F at $y = 0$. Note that a particular solution of Equation 37 is

$$F_P = \frac{1}{\sqrt{T - T'}} \exp \left[-\frac{y^2}{2(T-T')} \right] \text{ for } T > T' . \quad (44)$$

The integral over T' of this solution, multiplied by an arbitrary function of T' , is also a solution of Equation 37. Thus it can be verified that

$$F = 1 - \int_0^T \frac{H(T')}{\sqrt{T - T'}} \exp \left[-\frac{y^2}{2(T-T')} \right] dT' ; \quad (45)$$

is a solution for all T and y , except at the single point $y = 0$ where special limiting procedures will be used. Here $H(T')$ is an arbitrary function which we shall choose in order to satisfy the boundary condition (39).

The value of F at $y = 0$ is

$$F_1 = 1 - \int_0^T \frac{H(T')}{\sqrt{T - T'}} dT' . \quad (46)$$

The integral here is finite even though the integrand is singular at $T' = T$. Also, differentiating Equation 46 with respect to y , we have for finite y

$$\frac{\partial F}{\partial y} = \int_0^T H(T') \frac{y}{(T-T')^{3/2}} \exp \left[-\frac{y^2}{2(T-T')} \right] dT' . \quad (47)$$

In this equation we change the variable of integration from T' to

$$u = \frac{y}{\sqrt{2(T-T')}} , \quad T' = T - \frac{y^2}{2u^2} , \quad dT' = \frac{y^2}{u^3} du . \quad (48)$$

Equation 47 then becomes

$$\frac{\partial F}{\partial y} = 2\sqrt{2} \int_{y/\sqrt{2T}}^{\infty} H\left(T - \frac{y^2}{2u^2}\right) e^{-u^2} du . \quad (49)$$

We can now pass to the limit $y \rightarrow 0$ and find

$$\left. \frac{\partial F}{\partial y} \right|_{y=0} = 2\sqrt{2} H(T) \int_0^{\infty} e^{-u^2} du = \sqrt{2\pi} H(T) . \quad (50)$$

Thus using the boundary condition (39) we find

$$H(T) = \frac{1}{\sqrt{2\pi}} \frac{\beta}{1-T} F_1(T) . \quad (51)$$

Using this result in Equation 46 we obtain the integral equation for F_1 ,

$$F_1(T) = 1 - \frac{\beta}{\sqrt{2\pi}} \int_0^T \frac{F_1(T')}{1-T'} \frac{dT'}{\sqrt{T-T'}} . \quad (52)$$

The variable y has been eliminated. In the variable $x = 1/(1-T)$ this equation becomes

$$F_1(x) = 1 - \frac{\beta}{\sqrt{2\pi}} \int_1^x F_1(x') \frac{dx'}{\sqrt{x'(1-\frac{x'}{x})}} \quad (53)$$

SECTION 6
APPROXIMATE SOLUTION OF THE INTEGRAL EQUATION

For $T \ll 1$ we can find the approximate solution by iteration. Putting $F_1(T') = 1$ in the right hand side of Equation 52, we find for the first iteration

$$\begin{aligned}
 F_1(T) &\approx 1 - \frac{\beta}{\sqrt{2\pi}} \int_0^T \frac{dT'}{\sqrt{T - T'}} \\
 &\approx 1 - \sqrt{\frac{2}{\pi}} \beta \sqrt{T} \approx 1 - \sqrt{\frac{2}{\pi}} \beta \sqrt{x - 1} .
 \end{aligned} \tag{54}$$

This result verifies our expectation, Equation 41.

We can obtain this behavior for x near unity and have the asymptotic form (42) or (43) for large x if we try

$$F_1(x) = \frac{1}{(1 + A \sqrt{x - 1})^2} , \tag{55}$$

where A is a constant to be evaluated. In order to agree exactly with Equation 54, we would need to have

$$A = \frac{\beta}{\sqrt{2\pi}} \approx 0.4 \beta \quad (\text{for } x \text{ near unity}) , \tag{56}$$

but this may not be the best value for all x . Let us find the value of A which satisfies Equation 53 at $x = \infty$. Since $F_1(\infty) = 0$ we must have

$$\begin{aligned}
1 &= \frac{\beta}{\sqrt{2\pi}} \int_1^{\infty} \frac{dx}{\sqrt{x} (1+A\sqrt{x-1})^2} \\
&= \sqrt{\frac{2}{\pi}} \beta \int_1^{\infty} \sqrt{\frac{x-1}{x}} \frac{d(\sqrt{x-1})}{(1+A\sqrt{x-1})^2} \\
&= \sqrt{\frac{2}{\pi}} \beta \int_0^{\infty} \sqrt{\frac{u}{u+1}} \frac{du}{(1+Au)^2} .
\end{aligned} \tag{57}$$

Now we are interested chiefly in cases where β is small compared to unity. In these cases, A will have to be small in order to satisfy Equation 57. When A is small, most of the contribution to the integral comes from u such that $\sqrt{u/(u+1)} \approx 1$. Thus approximately,

$$1 \approx \sqrt{\frac{2}{\pi}} \beta \int_0^{\infty} \frac{du}{(1+Au)^2} = \sqrt{\frac{2}{\pi}} \frac{\beta}{A} . \tag{58}$$

Therefore we need

$$A \approx \sqrt{\frac{2}{\pi}} \beta \approx 0.8 \beta \quad (\text{for large } x) . \tag{59}$$

We may guess, to be verified later, that the best value of A is half way between the values (56) and (59), namely

$$A = 0.6 \beta \quad (\text{best guess}) . \tag{60}$$

SECTION 7
ACCURATE SOLUTION OF THE INTEGRAL EQUATION

Equation 52 can be solved by expansion of F_1 as a power series in \sqrt{T} . Let

$$v = \sqrt{T} , \quad (61)$$

and let

$$F_1(v) = (1-v^2)[1 + a_1v + a_2v^2 + a_3v^3 + \dots] . \quad (62)$$

Substituting in Equation 52 we find that the constant terms cancel, that (as in Equation 54)

$$a_1 = -\sqrt{\frac{2}{\pi}} \beta , \quad (63)$$

and that from the coefficient of v^{n+1}

$$a_{n+1} - a_{n-1} = -\beta b_n a_n , \quad (64)$$

where

$$b_n = \frac{1}{\sqrt{2\pi}} \int_0^v \frac{(v')^n}{v^{n+1}} \frac{2v' dv'}{\sqrt{v^2 - v'^2}} \quad (65)$$

$$= \sqrt{\frac{2}{\pi}} \int_0^1 u^{n+1} \frac{du}{\sqrt{1-u^2}} . \quad (66)$$

In writing Equation 64 we have canceled out a factor v^{n+1} , so this factor must appear in the denominator of Equation 65. The transformation to $u = v'/v$ made in going to Equation 66 then shows that b_n is a constant, so

that it was correct to factor out v^{n+1} . The integral in (66) can be made trigonometric by letting $u = \sin\theta$. We then obtain

$$b_n = \sqrt{\frac{2}{\pi}} \int_0^{\pi/2} (\sin\theta)^{n+1} d\theta . \quad (67)$$

These integrals are known. They are

$$b_0 = \sqrt{\frac{2}{\pi}} , \quad b_1 = \sqrt{\frac{\pi}{2}} \cdot \frac{1}{2} , \quad (68)$$

and in general

$$\left. \begin{aligned} b_n &= \sqrt{\frac{2}{\pi}} \frac{2 \cdot 4 \cdot 6 \dots n}{1 \cdot 3 \cdot 5 \dots n+1} \quad \text{for } n \text{ even} , \\ &= \sqrt{\frac{\pi}{2}} \frac{1 \cdot 3 \cdot 5 \dots n}{2 \cdot 4 \cdot 6 \dots n+1} \quad \text{for } n \text{ odd} . \end{aligned} \right\} \quad (69)$$

A property useful for calculations is that

$$b_{n+1} = \frac{1}{(n+2)b_n} . \quad (70)$$

The b_n decrease with increasing n ; for large n ,

$$b_n = \frac{1}{\sqrt{n + \frac{3}{2} + \frac{1}{8n} + \dots}} .$$

Thus the b_n can be calculated and, from Equation 64, the a_n . The latter alternate in sign, but increase without limit, although they increase more and move slowly with increasing n , becoming proportional to

$$a_n \sim (-1)^n \exp[\beta \sqrt{n + \frac{3}{2}}] . \quad (71)$$

The series in Equation 62 converges for all $v < 1$ but, unfortunately, only very slowly for v near unity (large x). While we know that the limit of the series exists as $v \rightarrow 1$, we have not yet been able to evaluate the limit and so obtain the asymptotic form of F_1 .

Because of the slow convergence of the series, we have solved the differential Equation 33 numerically for $\beta = 1, 0.3$ and 0.1 . The solid curves in Figure 2 were thus obtained by H. J. Longley.

The dashed curves in Figure 2 are computed from Equation 55 with A given by Equation 60, i.e.,

$$F_1(x) = \frac{1}{(1 + 0.6 \beta \sqrt{x-1})^2} . \quad (72)$$

As expected, this function is too small for small x and too large for large x , but the fit is not unacceptable. However, a much better fit to the computed curves is given by

$$F_1(x) = \frac{1}{[1+0.46\beta(x-1)^{0.59}]^2} . \quad (73)$$

The circles in Figure 2 are plotted from this formula. While it does not have the correct asymptotic form for very large x , it is quite accurate when the attenuation factor (F_1) is between 0.05 and 1, which is the range of practical interest. We shall therefore use it.

From the definitions (30) and (35) of x and β , we write our result (73) as

$$F_1(r,s) = \frac{1}{[1+s\tau_1]^2} , \quad (74)$$

where

$$\tau_1 = 0.46 \sqrt{\frac{r_0}{4\pi\sigma + \epsilon/\tau_1}} \left(\frac{r}{r_0} - 1\right)^{0.59} . \quad (75)$$

Here we have replaced ϵs by ϵ/τ_1 and regard the latter as independent of s . This equation is easily solved for τ_1 by iteration.

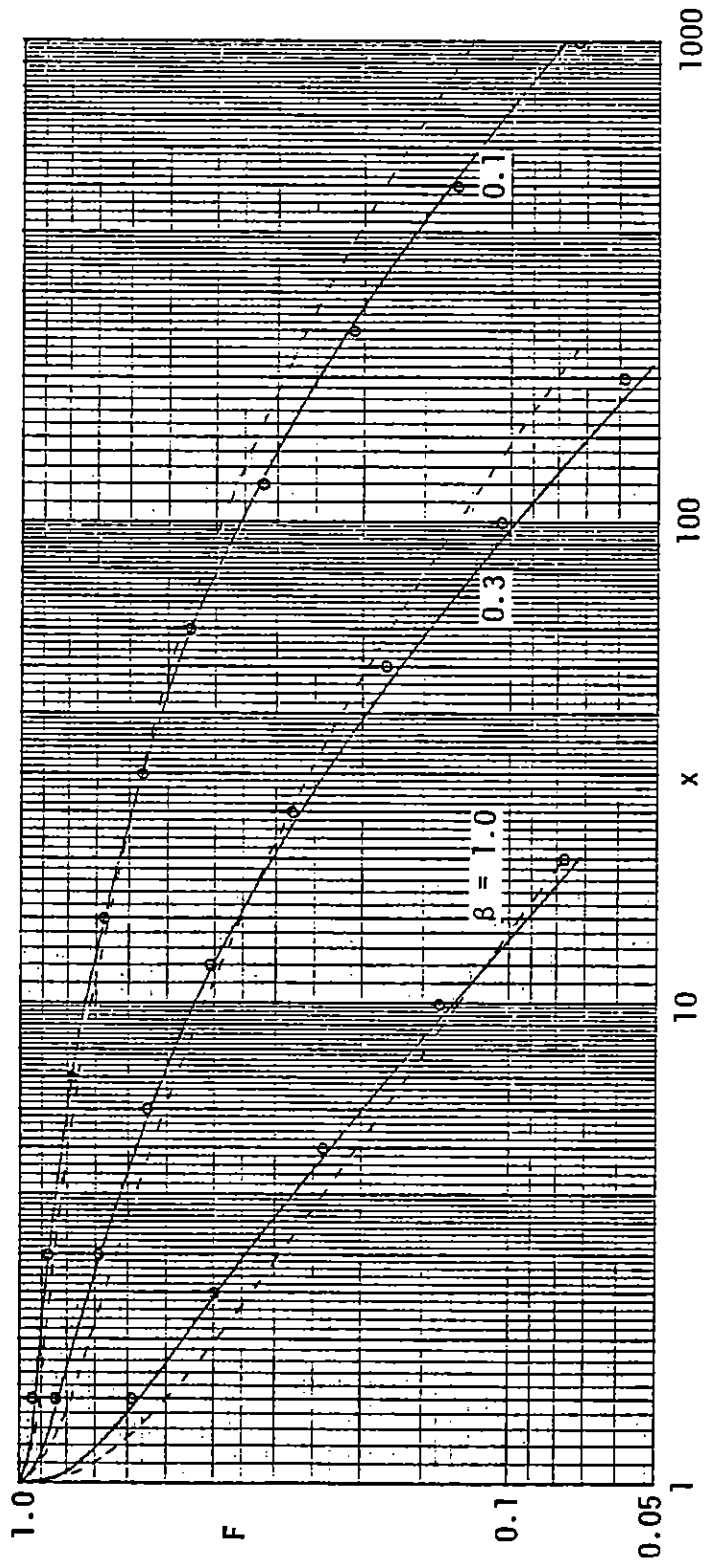


Figure 2. Comparison of various approximations to F. Solid curves, Longley's computed results. Dashed curves, approximate theoretical result, Equation 72. Circles, computed from fit, Equation 73.

SECTION 8
RESULTS IN TIME DOMAIN

Recall that $F_1(r,s)$ is the Laplace transform of the F field at the ground surface for an impulse function at $r = r_0$. But Equation 74 is the Laplace transform of the function

$$F_1(r,\tau) = \frac{\tau}{\tau_1} e^{-\tau/\tau_1}, \quad \tau > 0. \quad (76)$$

Therefore $F_1(r,\tau)$ is the impulse response in the time domain. Note that

$$\int_0^{\infty} F_1(r,\tau) d\tau = 1. \quad (77)$$

Thus the d.c. content is unaltered by ground attenuation; the EMP is simply smeared in time, over a time interval approximately equal to τ_1 .

Now let $E_0(r,\tau)$ be the vertical electric field on the ground as calculated by the LEMP extrapolation routine for the radius r , i.e., on the assumption of perfect ground conductivity. Then the field $E(r,\tau)$ corrected for finite ground conductivity is the convolution

$$E(r,\tau) = \int_{-\infty}^{\tau} E_0(r,\tau') \frac{d\tau'}{\tau_1} \frac{(\tau-\tau')}{\tau_1} e^{-(\tau-\tau')/\tau_1}. \quad (78)$$

Doing the convolution at each τ point is time consuming numerically. A much faster procedure is obtained by converting Equation 78 into two differential equations. By differentiating, we find

$$\frac{dE}{d\tau} + \frac{E}{\tau_1} = \frac{E_1}{\tau_1}, \quad (79)$$

where E_1 satisfies

$$\frac{dE_1}{d\tau} + \frac{E_1}{\tau_1} = \frac{E_0}{\tau_1}. \quad (80)$$

These two equations are easily integrated forward in τ , one integration step per output τ step, to give the corrected field.

SECTION 9
COMPARISON WITH SOMMERFELD SOLUTION

In 1909 Sommerfeld (Reference 4) solved the problem of a dipole radiating over a finitely conducting ground. His results are exact but difficult to evaluate numerically. Norton (Reference 5) has given an approximate evaluation which is quite accurate for typical soils. For soils which are good conductors, Norton's evaluation of F at the ground surface in the wave zone and in the Laplace domain is

$$F_N = 1 - \sqrt{\pi p_1} e^{p_1} \operatorname{erfc}(\sqrt{p_1}) , \quad (81)$$

where p_1 is the "numerical distance,"

$$p_1 = \frac{1}{2} \frac{s^2 r}{\epsilon s + 4\pi\sigma} = \frac{1}{2} \frac{r}{\lambda} \frac{1}{\epsilon + 4\pi\sigma\lambda} . \quad (82)$$

(Recall $\lambda = 1/s$ is the reduced wave length.) A good conductor is one for which $4\pi\sigma\lambda$ is somewhat greater than ϵ ; in typical cases, $4\pi\sigma\lambda/\epsilon \approx 5$, which is adequate. Also in typical cases,

$$\epsilon + 4\pi\sigma\lambda \approx 200 , \quad (83)$$

so that the wave zone corresponds to $p_1 \gtrsim 0.01$. The solid curve in Figure 3 represents F_N as a function of p_1 .

To compare our results with F_N , we have a choice of Equations 72 or 73. The latter is more accurate, but the former has simpler scaling properties; we therefore use (72). Note that

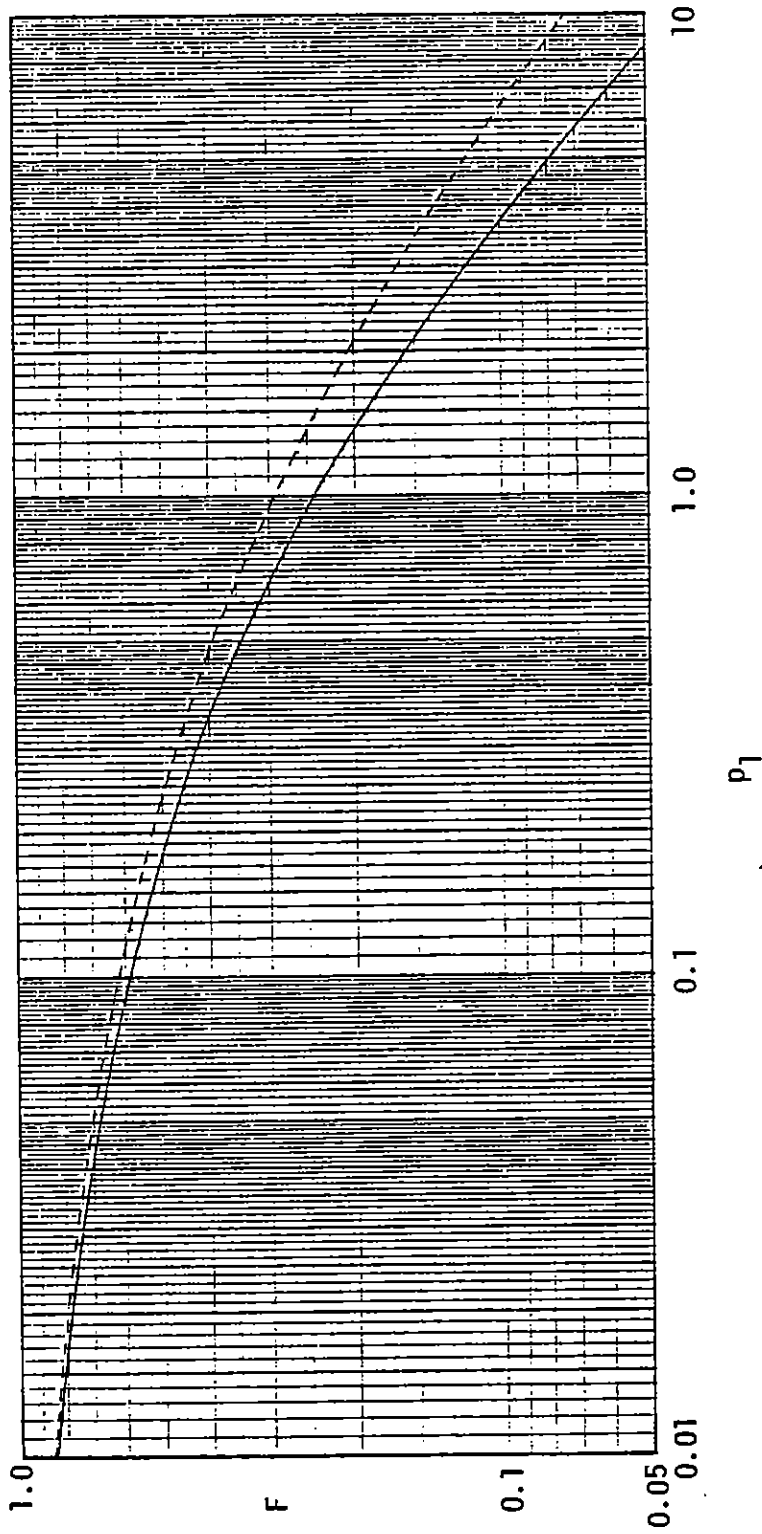


Figure 3. Comparison with Sommerfeld's results. Solid curve, Norton's evaluation of Sommerfeld's results, Equation 81. Dashed curve, our approximate theoretical result, Equation 87. Note that relation of dashed to solid curve is very nearly the same as in Figure 2.

$$0.6 \beta \sqrt{x - 1} = 0.6s \sqrt{\frac{r - r_0}{\epsilon s + 4\pi\sigma}} . \quad (84)$$

To apply to a dipole radiator, we should choose

$$r_0 \approx \lambda = 1/s . \quad (85)$$

Then in the wave zone we have $r \gg r_0$, and

$$0.6 \beta \sqrt{x - 1} \approx 0.6 \sqrt{\frac{s^2 r}{\epsilon s + 4\pi\sigma}} = 0.6 \sqrt{2p_1} , \quad (86)$$

and Equation 72 becomes

$$F_1 \approx \frac{1}{(1 + 0.6 \sqrt{2p_1})^2} . \quad (87)$$

The dashed curve in Figure 3 represents this formula.

We see in Figure 3 that the dashed and solid curves bear about the same relation to each other as those in Figure 2 for $\beta = 0.1$. In other words, the rough theoretical result (72) bears about the same relation to F_N as it does to our more accurate results. This implies that the correspondence of our approximate wave-zone theory with Sommerfeld's solution is good.

Let us estimate the value of β in this application. From Equations 85 and 35 we obtain

$$\beta = \frac{1}{\sqrt{\epsilon + 4\pi\sigma\lambda}} \approx 0.07 . \quad (88)$$

Thus it is satisfactory that the relation of the curves in Figure 3 be about the same as for the $\beta = 0.1$ case in Figure 2. It appears that the difference between F_N and our accurately calculated F_1 is no more than about 10 percent.

SECTION 10
HORIZONTAL ELECTRIC FIELD

From Equation 26 we can deduce the relation between E_r and the vertical field E_θ in the air just above the ground surface. This is

$$\begin{aligned} E_r &= -\sqrt{\frac{s}{\epsilon s + 4\pi\sigma}} E_\theta \\ &= -E_\theta / \sqrt{\epsilon + 4\pi\sigma\lambda}. \end{aligned} \quad (89)$$

It is not a bad approximation to regard the radical here as constant. Equation 29 shows that the vertical field E_z in the ground is down from E_r by another factor of the same radical ($\epsilon \gg 1$).

Actually, both ϵ and σ depend on s . A good representation of this dependence can be obtained from the universal soil model (Reference 6) by making the replacement $i\omega \rightarrow s$, which gives directly a real expression for $\epsilon s + 4\pi\sigma$ as a function of s . Then, in determining τ_1 from Equation 75, $\epsilon s + 4\pi\sigma$ should be evaluated self-consistently at $s = 1/\tau_1$; the self-consistent τ_1 can be found by iteration.

Similarly, in calculating E_r from E_θ by Equation 89, the factor $s/(\epsilon s + 4\pi\sigma)$ should be evaluated at $s = 1/\tau$; thus the ratio of E_r to E_θ depends on the retarded time τ to some extent.

Of course, more accurate fields could be obtained by using Fourier transforms and their inverses, at considerably more cost in computing time. For actual terrains we doubt that this would be worthwhile. In many cases of interest, the ground is not flat, and soil properties vary from place to place. For a burst in a bowl shaped valley, the ground attenuation can be negated, a point that should perhaps be studied.

REFERENCES

1. Longley, H. J., C. L. Longmire, J. S. Malik, R. M. Hamilton, R. N. Marks, and K. S. Smith, Development and Testing of LEMP 2, A Surface Burst EMP Code, MRC-R-272, Mission Research Corporation, December 1976, (unpublished).
2. Longley, H. J., C. L. Longmire, R. M. Hamilton, and R. N. Marks, SUB-L A Late-Time EMP Code, MRC-R-273, Mission Research Corporation, January 1977 (unpublished).
3. Dalich, S. J., and K. D. Granzow, Electromagnetic Pulse Environment Studies, AFWL-TR-73-286, Vol. 1, June 1974.
4. Sommerfeld, A., Ann. der Phys., Vol. 28, p. 665 (1909).
5. Norton, K. A., Proc. I. R. E., Vol. 24, p. 1367 (1936).
6. Longmire, C. L., and K. Smith, A Universal Impedance for Soils, MRC-N-214, DNA 3788T, Mission Research Corporation, October 1975.